

Reactive Plasticization of Poly(lactide) with Epoxy Functionalized Cardanol

Iulia Mihai,¹ Fatima Hassouna ,² Thierry Fouquet,³ Abdelghani Laachachi,¹ Jean-Marie Raquez,⁴ Hicham Ibn El Ahrach,¹ Philippe Dubois⁴

¹Materials Research and Technology Department, Luxembourg Institute of Science and Technology (LIST) –5, Rue Bommel, ZAE Robert Steichen, Hautcharage L-4940, Luxembourg

²Department of Chemical Engineering, University of Chemistry and Technology (UCT) Prague, Dejvice, 166 28, Czech Republic

³Research Institute for Sustainable Chemistry, National Institute for Advanced Industrial Science and Technology (AIST), Tsukuba 305-8565, Japan

⁴Laboratory of Polymeric and Composite Materials, Center of Innovation and Research in Materials and Polymers, CIRMAP, University of Mons, B-7000, Belgium

New biobased plasticizers made of di-functional glycidyl ether epoxy cardanol (ECard) were investigated to improve the ductility of renewable poly(lactide) (PLA). Compatibility between PLA and ECard was achieved out through *in situ* reactive grafting strategy catalyzed with Ethyltriphenyl phosphonium bromide (ETPB) using twin-screw extruder. In absence of catalyst, ECard forms domain ill-dispersed in the PLA matrix due to the high incompatibility between both phases. When ETPB is added as catalyst domain size distribution of the plasticizer decreased, indicating an enhanced compatibility due to the reactive grafting of a fraction of ECard plasticizer onto PLA backbone. Although all plasticized PLA specimens exhibit lower glass transition temperature, lower elastic/tensile modulus, lower yield stress, and higher strain at break, the reactive blend containing the lowest amount of catalyst, that is, 0.02 phr, exhibited the highest ductility behavior. POLYM. ENG. SCI., 58:E64–E72, 2018. © 2017 Society of Plastics Engineers

INTRODUCTION

Among biodegradable and biobased polymers available, poly(lactide) (PLA) is the most prevalent one on the market and cost-competitive compared to lots of conventional petroleum-based polymers. It has attracted growing interest in different markets, such as packaging, biomedical, electronic, and automotive industries [1–6]. Despite its numerous advantages such as high strength and high modulus, high optical properties, resistance to moisture and grease, flavor and odor barrier characteristics, biocompatibility, non-volatility, and nontoxicity, PLA presents some inherent brittleness, which limits its application [7]. Thus, PLA displays some drawbacks in terms of properties (poor impact strength, low elongation at break, low heat deflection temperature...) and processability [7]. PLA rigidity and

brittleness at room temperature are the result of its high glass transition temperature (T_g) close to 60°C [2]. Like most conventional glassy thermoplastics, the brittleness of PLA is due to strain- and stress-localizations when deformed below the brittle-to-ductile transition temperature, that is, under glass transition temperature. Under mechanical loading, PLA deforms via a highly localized strain and crazing mechanism [8]. To improve the properties of PLA, many strategies are already investigated including plasticization, polymer blending, copolymerization, surface modification [7, 9, 10]. Plasticization is commonly used to improve the processability of thermoplastics or to increase the flexibility as well as impact strength of glassy polymers [7, 9–11]. Several plasticizers for PLA are reported in the literature including cyclic lactides and oligolactic acids [12–14], bis-hydroxymethyl malonate (DBM) [15], glucose esters and fatty acid esters [16–19], citrates [14, 20], polyethylene glycol (PEG) [13, 15, 16], poly(propylene glycol) [21, 22], atactic poly(3-hydroxybutyrate) [18, 19], polyester diol as poly(diethylene adipate) [23], tributyl citrate-oligoester (TbC-oligoesters), diethyl bis-hydroxymethyl malonate oligoester (DBM-oligoester), and oligoesteramide (DBM-oligoesteramide) [15, 24, 25], modified soybean oil [16, 17]. Toughening through reactive extrusion with plasticizers such as PEG derivatives and citrate derivatives was also established [8, 16, 26–28].

Although blending PLA with plasticizers improves its mechanical properties, most of them are petroleum based compounds [16]. Hence, research towards a fully renewable plasticizer and therefore a fully renewable blend is of a high interest. The main goal of this study is to develop novel bioplasticizers that do not compromise the biodegradable and sustainable nature of PLA based materials at the same time as they can be produced in large scale from inedible biomass resources. Cardanol derivatives are thereby one of such renewable resource. Cardanol is a renewable and inexpensive organic natural resource that is obtained *via* the vacuum distillation of roasted cashew nut shell liquid obtained from the spongy mesocarp of cashew nut shells, a byproduct of cashew nut processing [29]. The chemistry of cardanol and its derivatives is becoming an interesting area in academic and industrial research, mainly for the preparation of new eco-friendly chemicals, composites, and functional organic materials [30, 31]. Indeed cardanol, is a mixture of 3-*n*-pentadecylphenol (20–30%), 3-(pentadeca-8-enyl)phenol (70–80%), 3-(penta-deca-8,11-dienyl)-phenol (nearly 5%), and

Additional Supporting Information may be found in the online version of this article.

Correspondence to: Dr. F. Hassouna; e-mail: fatima.hassouna@vscht.cz

Contract grant sponsor: Science Policy Office of the Belgian Federal Government (PAI 7/5); contract grant sponsor: European Commission/Walloon Region (FEDER – BIORGEL RF project – Valicell); contract grant sponsor: Belgian National Fund for Scientific Research (FNRS).

DOI 10.1002/pen.24647

Published online in Wiley Online Library (wileyonlinelibrary.com).

© 2017 Society of Plastics Engineers

3-(pentadeca-8,11,14-trienyl) phenol (<5%) [30]. Specific properties of cardanol and its derivatives, such as the relatively high solubility in nonpolar milieu and good processability, can be attributed to the presence of the -C15- chain attached to the meta position of the phenolic ring [30]. Cardanol and its derivatives find major applications in biocomposites, synthetic resins, epoxy curing agents, and coatings [31, 32]. Recently, cardanol has been used as a plasticizer for poly(vinyl chloride) and rubber, with or without chemical modification, and has revealed significant plasticizing effects [32, 33].

Epoxidized cardanol (ECard) is one of such cardanol derivatives, which is produced on an industrial scale and is being used for polymers, coatings, and adhesives. Recently, some of us have synthesized a novel cardanol-derived plasticizer, that is, methoxylated hydroxyethyl cardanol, through methoxylation of the double bonds on the side chain of cardanol (C15 chain thus attached to the meta position of the phenolic ring) [34]. The plasticization efficiency of methoxylated hydroxyethyl cardanol was demonstrated by a substantial decrease of the glass transition temperature and storage modulus together with a significant increase of the elongation at break as compared with neat PLA. Moreover, methoxylated hydroxyethyl cardanol exhibited higher plasticization performance than the commercial hydroxyethyl cardanol (pCard) toward PLA.

Interestingly, reactive extrusion has proven to be an ecological, cost effective, and versatile process to design novel and high performance bioplastics. In the present study, the potential for application of ECard as plasticizer for PLA is investigated. *In situ* reactive grafting strategy has been employed to improve the compatibility between PLA and ECard using co-rotating twin-screw extruder. The reactive plasticization effect on the chemical structure, morphology, thermal, and mechanical properties of PLA/ECard was evaluated.

EXPERIMENTAL

Materials

PLA (4042D) was supplied by NatureWorks LLC (Minnetonka, USA). Epoxidized cardanol (ECard) NC-514 S Cashew Liquid Resin was obtained from Cardolite Chemical Zhuhai CO (Guangdong, China) and used as supplied. Ethyltriphenyl phosphonium bromide (ETPB) and chloroform were purchased from Sigma Aldrich (St Louis, MO) and used as received.

Processing

Several compositions were prepared using a 15 cc twin-screw micro-extruder DSM XPlore with *L/D* ratio 18 (Geleen, The Netherlands). The following PLA/ECard/ETPB materials were considered as: 100/0/0 (wt%), 80/20/0 (wt%), 80/20/0.02 phr (per hundred parts of resin), 80/20/0.06 phr, and 80/20/0.1 phr. In fact, the amount of plasticizer ECard was fixed to 20% after an optimization step. The processing conditions were also set up after an optimization step. Therefore, the barrel temperature was set at 180°C, screw speed was fixed to 100 rpm and the residence time to 5 min. PLA pellets were first dried overnight at 50°C before processing. PLA was first introduced and melted in the preheated micro-extruder. Dry ECard and ETPB were mixed and then injected into the extruder using a syringe.

Standard samples of the resulting materials were then prepared by injection molding machine (Model HAAKE MiniJet II, Thermo Scientific) at 180°C and 700 bar during 5 s.

Characterization

Fourier-Transform Infrared (FTIR) Spectroscopy . The changes in the chemical structure of PLA were evaluated by FTIR spectroscopy in attenuated total reflectance mode from 400 to 4000 cm^{-1} using a Bruker Optics Tensor 27 spectrometer.

Differential Scanning Calorimetry (DSC) . DSC measurements were performed on Netzsch DSC 204 F1 instrument (Selb, Germany) under nitrogen gas flow, with a heating rate of 10°C min^{-1} . Samples (5–10 mg) were sealed in hermetic aluminum pans and were subjected to the following temperature program: (i) a first heating step from –100 to 200°C, (ii) a cooling step from 200 to –100°C, and (iii) a second heating step from –100 to 200°C. T_g values were measured at the second ramp. The second heating eliminates the uncertainties due to the thermal history of the materials and therefore allows evaluating the inherent properties of the materials.

Size Exclusion Chromatography . Molecular weight change analyses were conducted with Agilent Technologies series 1200 operating with a differential refractive index detection and a linear column (PLgel Mixed-D 5 and 3 μm , 200 Da < Mw < 200 kDa in chloroform 1 ml min^{-1}). Sample preparation was performed by dissolving the material to be analyzed in chloroform at a concentration of 2 mg ml^{-1} . This was followed by the filtration of the prepared material solution using a syringe and an acrodisc-branded filter (pore size 0.45 μm). All analyses were run at room temperature.

For SEC analyses with UV detection, the apparatus consisted of 600E controller & pumping units (Waters, Versailles, France) followed by 486 tunable UV/Vis detector (Waters). Separation was performed on a unique mixed bed column (PLgel Mixed-D 300 \times 7.5 mm, particle size 5 mm, Agilent) with precolumn (PLgel Mixed-D 50 \times 7.5 mm) at room temperature. THF was used as eluent at a flow rate of 1 ml min^{-1} . Twenty microliters of a 1 and a 15 g L^{-1} resin solution were injected for SEC and SEC-SALDI analyses with satisfactory *S/N* ratio in a single run, respectively.

Thermogravimetric Analysis . Thermal stability of the plasticized PLA materials was investigated by means of thermogravimetric analyzer (TGA) model STA 409PC from NETZSCH; [15–20] mg of sample in an aluminum pan was heated from room temperature up to 600°C under air (100 ml min^{-1}) gas flow. The runs were carried out in dynamic conditions at a heating rate of 10°C min^{-1} .

Scanning Electron Microscopy (SEM) . Microstructure of plasticized PLA materials was studied by means of pressure controlled SEM Quanta Field Effect Gun 200 from FEI (Eindhoven, The Netherlands). To this end, all samples were fractured after immersion in liquid nitrogen for about 5 min to observe the fracture surface of the materials.

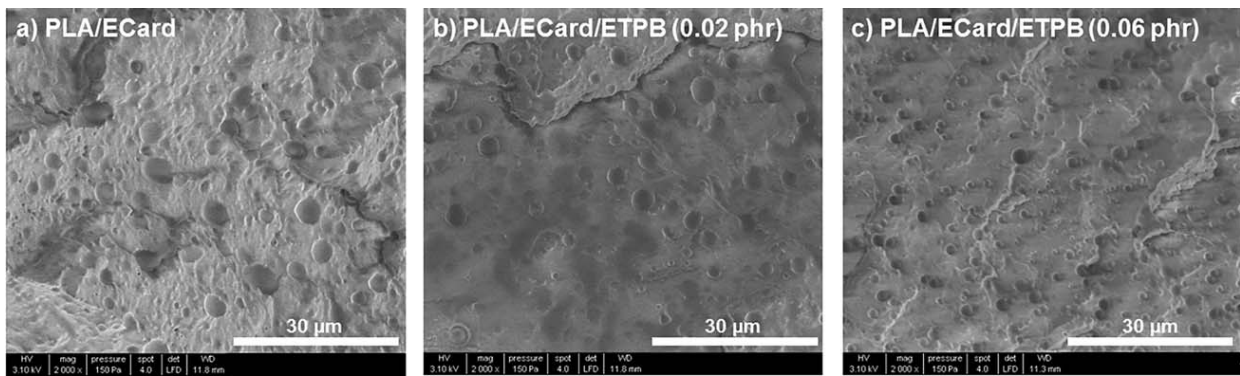


FIG. 1. SEM images of a) PLA-ECard, b) PLA- PLA-ECard-ETPB 0.02 phr, c) PLA-ECard-ETPB 0.06 phr.

Dynamic Mechanical Analysis (DMA). The viscoelastic properties were evaluated by means of DMA using a Netzsch equipment model DMA 242C. Rectangular specimens ($60 \times 11 \times 3 \text{ mm}^3$) were used. They were conditioned for at least 24 h at 20°C and 50% of relative humidity before testing. Subsequently, they were subjected to double cantilever mode of flexural loading with amplitude of $30 \mu\text{m}$ in the temperature range from -60 to 120°C at a heating rate 2°C min^{-1} and a frequency of 1 Hz.

Tensile Tests. The quasi-static uniaxial tensile testing was done with a universal testing machine Instron model 5967 (Norwood, MA). Tensile specimens based on ASTM D638 with sample type V were used. The specimen had an overall length of 63.5 mm and a thickness of 3 mm. The gauge section of the specimen had a length of 25 mm and a minimum width of 3 mm. The specimens were conditioned for at least 24 h at 20°C and 50% of relative humidity before testing. The engineering axial stress versus axial strain curves were recorded at room temperature at a constant crosshead rate of 1 mm min^{-1} until break.

RESULTS AND DISCUSSION

Reactive Extrusion Modification and Plasticizing of PLA

In situ reactive grafting strategy has been employed to improve the compatibility between PLA and ECard by reactive extrusion.

Figure 1 shows the SEM images of the PLA-ECard blends. In absence of ETPB, ECard forms microsized domains dispersed in the PLA matrix (Fig. 1a). ECard domain average size is about $5 \mu\text{m}$. The weakness of the interface between PLA and ECard is evident, highlighting a high incompatibility between both phases. In order to decrease ECard domain size and strengthen the interface between PLA and the plasticizer, ETPB was added as a catalyst [35]. Indeed, the epoxide groups present in Ecard chemical structure can react either with $-\text{COOH}$ or with $-\text{OH}$ of the PLA end groups under the catalytic effect of ETPB to form some grafted copolymer that can function as compatibilizer between PLA and ECard. The grafting of a fraction of ECard plasticizer onto PLA backbone by reactive extrusion is expected to lead to the creation of more interactions between the so-functionalized polyester matrix and the remaining fraction

of nongrafted plasticizer [26, 27]. Therefore, different concentrations of ETPB were introduced into PLA/ECard blend and their effect was investigated.

Figure 1b and c show that the domain size distribution of the plasticizer decreases in presence of ETPB. This decrease is accentuated with the increase of the catalyst amount (3 and $1 \mu\text{m}$ in presence of 0.02 and 0.06 phr, respectively). This morphological trend can be explained by a grafting of a fraction of ECard plasticizer onto PLA backbone by reactive extrusion leading to the creation of more interactions between the so-functionalized polyester matrix and the remaining fraction of nongrafted plasticizer. The grafting rate being proportional to the amount of ETPB, it has a direct impact on the domain size distribution of the plasticizer.

Grafting of ECard plasticizer onto PLA backbone by reactive extrusion was characterized by FTIR and SEC-MALDI-MS. Figure 2 shows the FTIR spectra within the region of epoxy absorption. The intensity of the peak at 912 cm^{-1} attributed to epoxy groups of ECard decreases markedly with the addition of ETPB, suggesting reactions of epoxy groups during the reactive extrusion [35]. The reaction mechanism of $-\text{COOH}$ and $-\text{OH}$

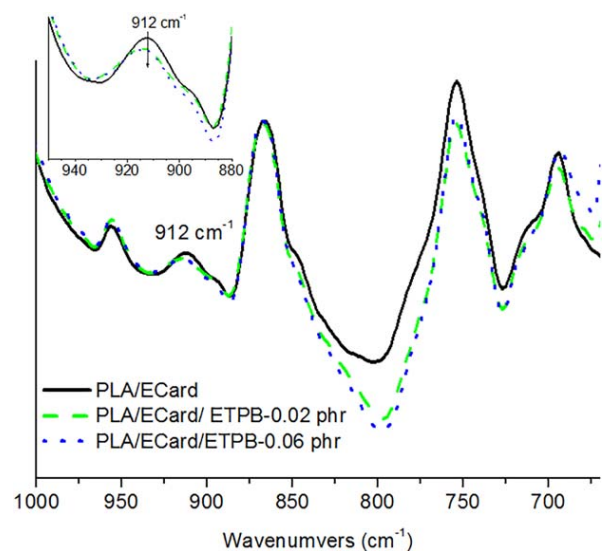
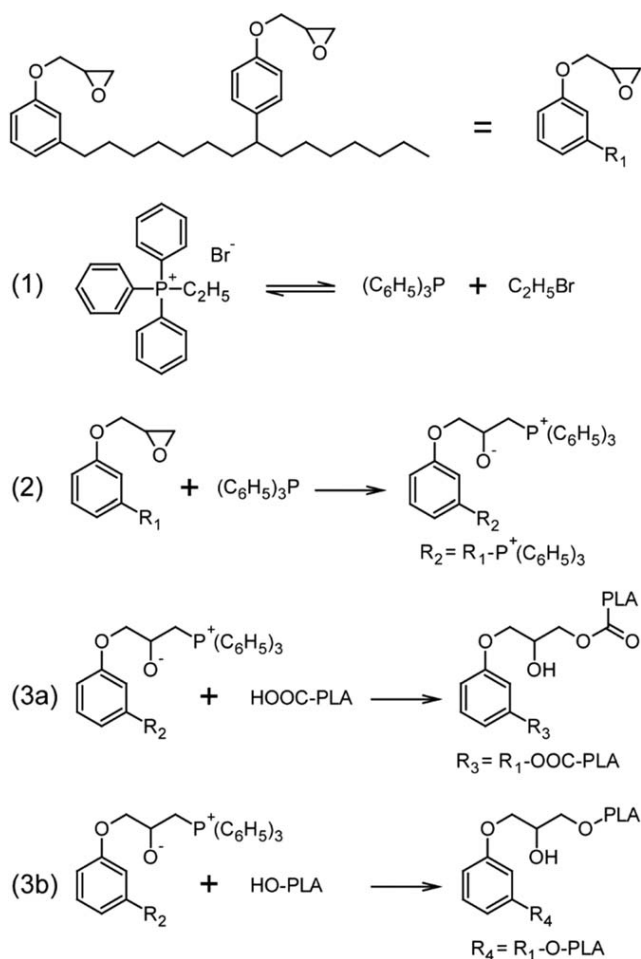


FIG. 2. FTIR spectra of plasticized PLA-based materials.



SCHEME 1. Reaction of PLA end groups with Ecard under the catalytic effect of ETPB.

groups with epoxy groups in presence of catalysts is already established [36]. It is established that ETPB dissociates easily under the mixing conditions and proceeds through a nucleophilic attack, which opens the epoxy ring in Ecard to generate an intermediate product. This product has high reactivity toward $-\text{COOH}$ and $-\text{OH}$ of PLA end chain groups, leading to the formation of PLA-g-Ecard copolymer. It is expected that the formed copolymer can act as an efficient compatibilizer for PLA/Ecard blends. The reaction scheme for Ecard with PLA in presence of ETPB is shown in Scheme 1.

In addition to FTIR characterization, SEC analyses were also conducted on a device equipped with a UV detector. Cardanol moiety is indeed UV active at 280 nm [37] while PLA is transparent at such wavelength. Since PLA is of higher molecular weight than Ecard, any peak detected at a short retention time in the SEC chromatogram of a PLA/Ecard/ETPB sample would highlight any grafting of cardanol on the PLA backbones. As compared to the SEC chromatogram of Ecard (Fig. 3a), the chromatograms of three PLA/Ecard/ETPB 80/20/ X samples with $X = 0.02$ (Fig. 3a), $X = 0.06$ (Fig. 3b) and $X = 0.1$ (Fig. 3c) display a distinct broad peak detected in the shortest elution volumes ($\sim 6\text{--}9$ ml), validating the presence of high molecular weight compounds bearing UV-active groups. The two main peaks at the longer retention times are assigned to epoxidized

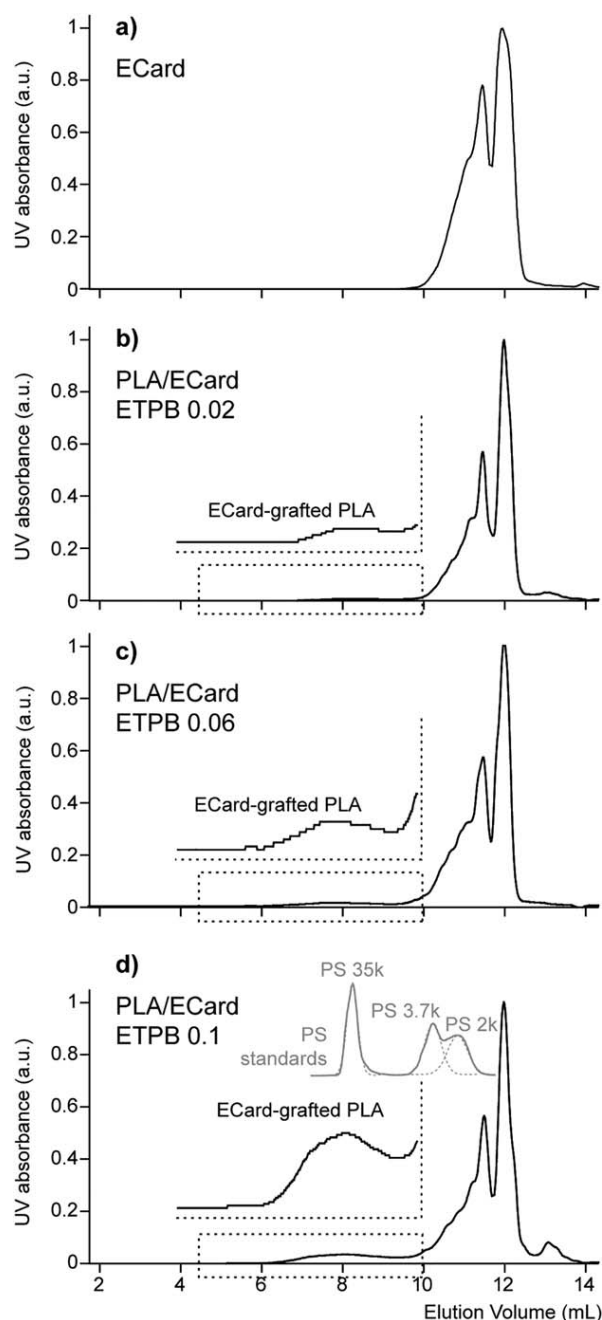


FIG. 3. SEC chromatograms of (a) Ecard and PLA/Ecard/ETPB in THF (b) 80/20/0.02, (c) 80/20/0.06, and (d) 80/20/0.1 recorded using a UV detector set at 280 nm. Insets in (b–d) Ecard-grafted PLA peaks (normalized). The SEC chromatogram of a mixture of three PS standards 35,000, 3,700, and 2,000 g/mol (UV detection, 254 nm) is depicted in inset of d).

cardanol and dimers as already characterized for NC514 [37] (NC514S named Ecard in this work is a purified grade of NC514—see Figure S1 in the Supporting Information—but of similar chemical nature). Note that the decrease of intensity of the dimer peak for the three formulated samples are compared to the pristine Ecard. Dimers contain more epoxy groups and are more prone to react with PLA than the monomer of Ecard.

The SEC elution of three PS standards 35,000, 3,700, and 2,000 g mol⁻¹ is depicted in inset of Fig. 3d (light gray line). The PS 35,000 g mol⁻¹ standard and the Ecard-grafted PLA

TABLE 1. Molecular weights and dispersity as determined by SEC on all the investigated materials.

Blend composition (W/W)	\bar{M}_n (g/mol) (PS)		\bar{M}_w (g/mol) (PS)		Dispersity \bar{D} (M_w/M_n)	
	PLA	ECard*	PLA	ECard*	PLA	ECard*
Extruded PLA	118,120		244,280		2	
Ecard		756		1,188		1.5
PLA/ECard (80/20)	113,460	793	224,540	1,266	2	1.5
PLA/ECard/ETPB (80/20/0.02 phr)	105,570	799	217,260	1,271	2	1.5
PLA/ECard/ETPB (80/20/0.06 phr)	91,500	682	182,000	1,106	2	1.5
PLA/ECard/ETPB (80/20/0.1 phr)	51,700	691	101,000	1,125	2	1.5

peak maxima have similar retention volumes (~ 8.1 ml), while the PLA peak is broad and some species elute in a much shorter time. The molecular weight of these polymeric chains thus ranges approximately between 100,000 and 20,000 g mol^{-1} (PS equivalent) and could thus be seen as “intact” PLA backbones carrying epoxidized cardanol grafted on the end-group(s) upon ring opening of the epoxy group. One should also note the increase of the relative abundance of the ECard-PLA peak with the increase of the catalyst molar ratio (from 0.02 to 0.1) as evidenced in the insets of Fig. 3b–d. Increasing the amount of initiator tends to favor the grafting of the epoxidized cardanol in a noticeable extent under relatively given molar ratio limits. An attempt has been conducted using a PLA/ECard/ETPB formulation at 80/20/0.1. The appearance of the extruded mixture strongly suggested the PLA has been degraded. Its SEC chromatogram depicted in Figure S2a (Supporting Information) confirms this observation with a broad peak convoluted with the oligomers of ECard readily detected with an associated molecular weight comprised between 30,000 and 1,500 g mol^{-1} (according to the elution volumes of the PS standards, inset in Figure S2a). A SEC-MALDI-MS coupling on this last PLA/ECard/ETPB 80/20/0.1 assessed the PLA nature of the broad polymeric distribution by the 72 Da shift between consecutive oligomers ($\text{C}_3\text{H}_4\text{O}_2$, the repeating unit of a PLA chain). The degradation of the PLA sample, i.e. cleavage of bonds upon thermo-oxidative processes leading to the mass reduction, and the complexity of ECard (expected to be a diepoxidized cardanol but most likely containing residual phenol groups instead of epoxy and dimers as impurities [37] account for the occurrence of several mass distributions. The detection of a complex isotopic pattern for each oligomer in Figure S2c is in accordance with the presence of at least one cardanol moiety along the backbone (consecutive peaks spaced by 2 Da owing to the polyunsaturated side chain [38] constituting a preliminary clue at a molecular level for the grafting of NC514S on PLA chains.

In addition to the SEC analyses conducted on device equipped with a UV detector to highlight the reactive grafting of ECard onto PLA backbone, SEC analyses were also conducted on another device equipped with RI detector to check at any changing of the molecular weight of PLA. SEC analyses used to determine the apparent molecular weight (M_n and M_w) of all samples according to polystyrene standards are summarized in Table 1.

Melt blending of PLA with 20 wt% of ECard does not have any impact on PLA molecular weight. The addition of 0.02 phr of ETPB does not affect the molecular weight of the polymer when taking into account the uncertainty of SEC measurements (ca., 10%). However, for higher ETPB concentrations (>0.02

phr), a significant shift of M_w and M_n toward lower molecular weights is observed, thus highlighting a concordance with the results obtained with SEC-MALDI-MS. The presence of high amount of catalyst leads to PLA chain scissions. PLA chain scissions can be attributed to a nucleophilic attack of the dissociated ETPB species under melt blending as explained above.

Besides the chain scission mechanism, branching/crosslinking reactions also occur during the reactive extrusion. The branching/crosslinking can be explained by the presence of difunctional epoxy groups in ECard, which can play a role of crosslinker. The crosslinked moiety could not be analyzed by SEC as it became insoluble [35].

Therefore, an excessive amounts of catalyst is not recommended as it can have a negative impact on PLA molecular weights.

Overall, the morphological analysis combined with FTIR and SEC-MALDI-MS show that the addition of ETPB catalyst leads to the creation of PLA-*g*-ECard copolymer. This latter takes an effective role in compatibilizing PLA/ECard. Even though the increase of the catalyst content has a positive impact on the enhancement of the compatibility between the polymer and the catalyst, it is clearly shown that at higher catalyst content (>0.02 phr), PLA chain scission occurs, therefore deteriorating the overall properties of PLA based materials.

Thermal Behavior

TGA and DSC were used to examine the thermal properties of all PLA based materials after melt processing.

The effect of the plasticizer on the thermal stability of the polymeric matrix is not often considered when studying plasticization of polymers. To investigate the effect of the presence of

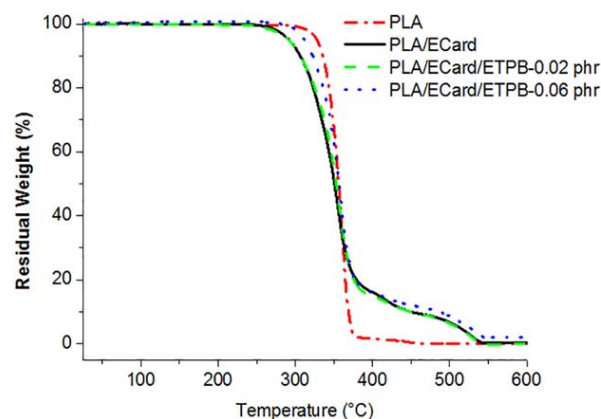


FIG. 4. TG curves for neat and plasticized PLA-based materials under air atmosphere.

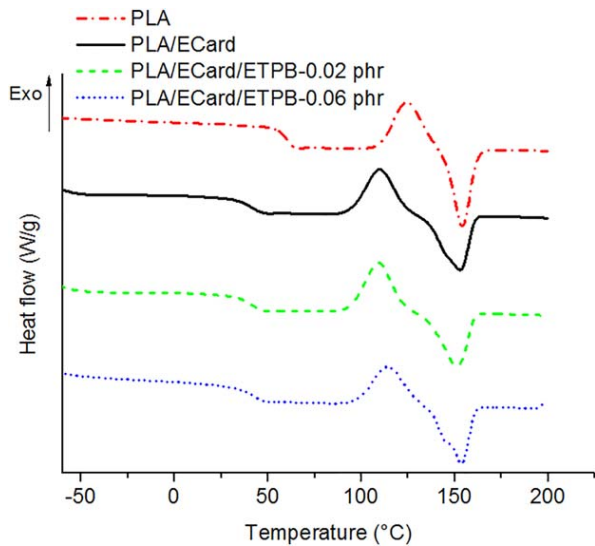


FIG. 5. DSC curves recorded for neat and plasticized PLA-based materials during the second heating.

ECard and the reactive grafting of a fraction of this latter on the thermal stability of PLA matrix, TGA measurements were performed on the elaborated formulations (Fig. 4). The thermal stability of plasticized PLA was compared with that of neat PLA. Figure 4 shows the TG curves for PLA and plasticized PLA with ECard in absence and in presence of ETPB (0, 0.02, and 0.06 phr). The addition of ECard to PLA matrix leads to a slight shift of the decomposition onset temperature to lower temperatures with respect to neat PLA. However, the reactive grafting of a fraction of ECard onto PLA backbone after addition of 0.02 phr of catalyst does not seem to have any impact on the thermal decomposition temperature of plasticized PLA as compared with the nonreactive system PLA/ECard. However, in a highly reactive system containing 0.06 phr of catalyst, a lower decrease of the decomposition onset temperature is displayed. This could be due to the PLA molecular mobility restriction caused by high grafting rate of ECard. However, it should be noted that no effect related to the presence of ECard and its reactive grafting on PLA backbone was observed on the decomposition temperature at 50% weight loss. Overall, the addition of ECard in absence and in presence of catalyst did affect the thermal stability of PLA only at higher temperature ranges

(above 270°C), which are far away from the temperatures used during the melt processing.

Thermal behaviors of the investigated PLA/ECard materials were examined by means of DSC. Table 2 and Fig. 5 summarize the thermal properties of neat and plasticized PLA.

DSC thermogram of neat PLA displays a glass transition temperature (T_g) at about 60°C, an exothermic peak of cold crystallization around 124°C and an endothermic melting peak at 154°C. Furthermore, the melting enthalpy (ΔH_m) of neat PLA is about equal to the enthalpy of cold crystallization (ΔH_{cc}), indicating that neat PLA is entirely amorphous. This is due to the fact that the investigated PLA contains 4.6% of D-lactide isomer, which reduces its capability to crystallize.

The addition of 20 wt% ECard leads to the shift to lower values of the glass transition and the cold-crystallization peak ($T_g = 41^\circ\text{C}$, $T_{cc} = 110^\circ\text{C}$). This shift is probably due to enhanced PLA chain mobility as a consequence of the presence of a high amount of low molecular weight plasticizer. Moreover, besides the main melting peak (T_m) at 153°C, a shoulder at 142°C appeared. Multiple melting peaks are typically observed in semi-crystalline polymers due to melt-recrystallization, and for PLA, corresponds to melting of initial lamellae and that of thicker, more perfected crystals formed during heating [39]. In this particular case, in the presence of ECard, this is directly linked to an increased mobility for short-range motion of the PLA chains. As a consequence a large portion of the amorphous phase got allowed to crystallize in the plasticized PLA [24], demonstrated by the presence of the shoulder (142°C) in the melting peaks of PLA blends. The reactive grafting of a fraction of ECard in presence of 0.02 phr of catalyst does not affect the overall thermal properties of plasticized PLA as T_g , T_{cc} , and T_m remained constant. However, even though no sensitive evolution is observed on the T_g and T_m of the reactive blend containing three times more of catalyst (0.06 phr), T_{cc} did shifted toward higher values (114°C). The evolution of T_{cc} as a function of the presence of ECard and catalyst is as follows: $T_{cc}\text{-PLA} > T_{cc}\text{-PLA/ECard/ETPB-0.06 phr} > T_{cc}\text{-PLA/ECard} \approx T_{cc}\text{-PLA/ECard/ETPB-0.02 phr}$. The origin of this trend is not clear as many processes occur at the same time during reactive extrusion (grafting, branching, crosslinking, chain scission...). However, two explanations can be stated out: (i) It is known from the literature that grafting may increase the crystallization temperature as the result of increased chain interaction, making it more difficult for these chains to disentangle from each other to crystallize

TABLE 2. Overall thermal and mechanical properties of all the materials investigated.

Blend composition (in wt%)	T_g^a (°C)	T_{cc}^a (°C)	T_m^a (°C)	$(\Delta H_m - \Delta H_{cc})^a$ (J/g)	T_g^b (E''_{max}) (°C)	E^c (MPa)	E_t^d (MPa)	σ_y^d (MPa)	ε_b^d (%)
Extruded PLA	60	124	154	0	60	1,850	1,861	63	5.7
Epoxidized Cardanol (ECard)	-46	-	-	-	-	-	-	-	-
PLA/ECard 80/20	41	110	153	2.2	-45 and 50	1,488	1,361	28	32
			144						
PLA/ECard/ETPB (80/20/0.02 phr)	41	109	153	2.8	-45 and 46	1,377	1,110	34	49
			143						
PLA/ECard/ETPB (80/20/0.06 phr)	41	114	154	0.5	-45 and 46	1,510	1,425	31	11
			145						

^aGlass transition temperature from the second heating DSC scans.

^bGlass transition temperature at maximum E'' (DMA).

^cStorage modulus at 20°C (DMA).

^dTensile properties at 20°C according to ASTM D638 (test speed 5 mm min⁻¹).

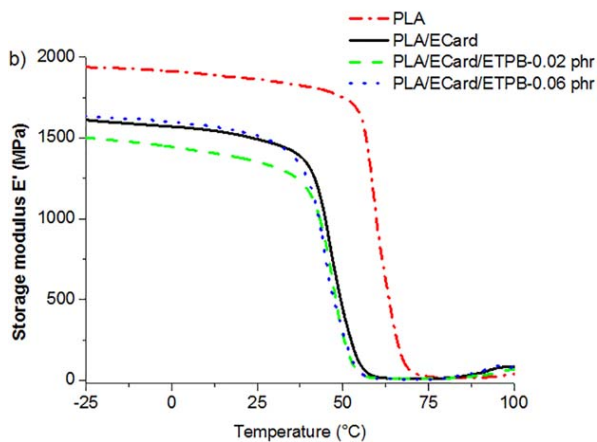
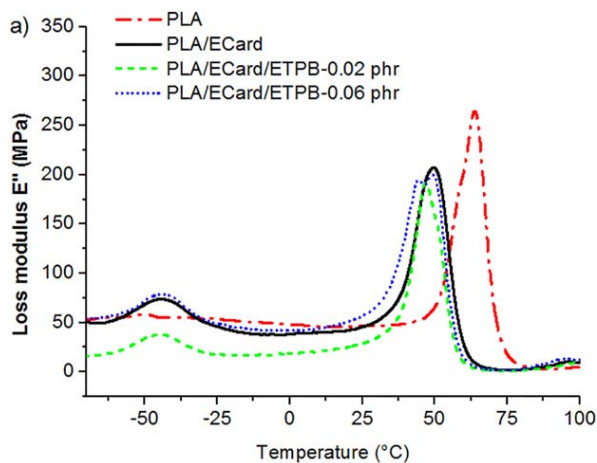


FIG. 6. Temperature dependence of (a) loss modulus E'' and (b) storage modulus E' for neat and plasticized PLA-based materials.

[40]. In the systems PLA/ECard/ETPB, this trend is observed only in the most reactive blend (at high grafting rate). (ii) ECard, being a difunctional glycidyl ether epoxy cardanol, crosslinking/branching reactions should take place simultaneously between the epoxy groups of the plasticizer and the carboxyl and hydroxyl end groups of PLA chains during reactive extrusion. As a consequence, the ability of PLA chains to crystallize can be hindered.

Mechanical Properties

Dynamic mechanical measurements were performed at 1 Hz to reveal the impact of plasticization and reactive grafting of ECard on the mechanical characteristics of the blend. The temperature effect on the storage modulus E' and loss modulus E'' is depicted Fig. 6a and b and the extracted mechanical parameters are summarized in Table 2 for neat and plasticized PLA. T_g values are defined as the temperature of the maximum of the loss modulus (E'') obtained for α relaxation.

Neat PLA exhibits one T_g equal to 60°C while all plasticized blends display two distinct T_g , indicating the occurrence of a phase-separation. The first T_g , is equal to -45°C for free Ecard, while the second value above 40°C corresponds to the T_g of plasticized PLA chains. Plasticized PLA chains in all blends display lower T_g as compared with neat PLA. Moreover, unlike DSC

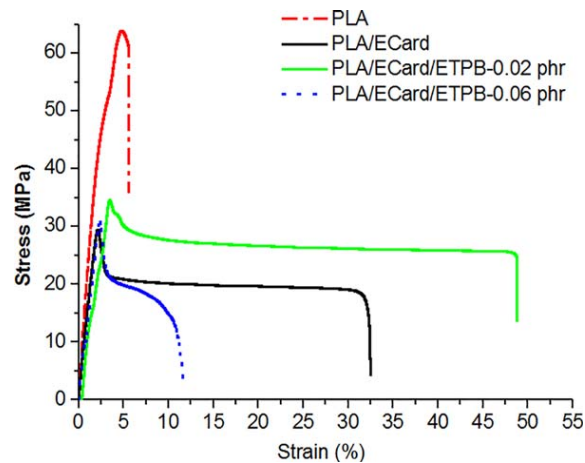


FIG. 7. Tensile strain-stress curves for neat and plasticized PLA-based materials.

results, DMA shows the reactive grafting effect of ECard on the T_g of the blends. Indeed, the reactive systems PLA/ECard/ETPB display lower T_g (46°C) than the nonreactive one PLA/ECard ($T_g = 50^\circ\text{C}$). Similar behaviour was observed in our previous study, in which the reactive blend PLA + 10% MAG-PLA + 20% PEG [MAG-PLA: anhydride grafted PLA, PEG: poly(ethylene glycol)] displayed lower T_g as compared with the nonreactive one PLA + 20% PEG [26]. It is commonly admitted that the glass transition implies cooperative motions in one chain that are governed by intramolecular interactions as well as by intermolecular interactions [41]. A certain dynamic free volume is required allowing conformational change of the chain. Therefore, further decrease of T_g in the reactive blend can be caused by the enhancement of PLA chain disentanglement due to the presence of PLA-g-ECard which will space out the chains, thereby leading to the expansion of the free volume. The conformation of PLA-g-ECard formed during the reactive extrusion can be at the origin of the increase of PLA chain disentanglements. Physical interactions between grafted and free ECard could be also considered when describing the decrease of the T_g . Indeed, as discussed above, the formation of PLA-g-ECard copolymer improves probably the interfacial adhesion and the compatibility in PLA blends and thus the plasticizing efficiency of ECard.

As stated by Piorkowska et al. [42], the curve loss modulus E'' – temperature gives information about the dispersion/distribution of ECard within amorphous PLA phase. The existence of an additional low temperature peak in the plasticized PLA suggests the formation of ECard-rich phase. Moreover, a broadening of the width of the peak reflecting the glass transition is due to a plasticizer concentration gradient in all PLA blends.

Differences in results observed between DSC and DMA are in general due to the fact that these two techniques are based on different solicitation modes and thus their results cannot be systematically compared.

When looking at the storage modulus E' curves as a function of temperature for neat and plasticized PLA (Fig. 6b and Table 2), one can notice that E' measured at 20°C, for neat PLA is higher (1850 MPa) than that of the plasticized blends. However, among the plasticized blends, the reactive blend containing the lowest amount of catalyst, that is, 0.02 phr, displayed the lowest storage modulus (1377 MPa). When increasing the content of

the catalyst, that is, 0.06 phr, the storage modulus of the material increased from 1377 MPa (PLA/ECard/ETPB-0.02 phr) to 1510 MPa. Therefore, the evolution of E' as a function of the presence of Ecard and catalyst is as follows: E' -PLA > E' -PLA/ECard/ETPB-0.06 phr > E' -PLA/ECard > E' -PLA/ECard/ETPB-0.02 phr. A clear correlation between the increase of E' and the increase of T_{cc} in the most reactive blend, that is, PLA/ECard/ETPB-0.06 phr as compared with PLA/ECard/ETPB-0.02 phr can be made. Even though these two reactive blends display the same T_g according to DSC and DMA, they do exhibit different viscoelastic properties.

Nominal tensile axial stress-strain behavior at room temperature, 20°C, of neat and plasticized PLA materials is depicted Fig. 7. The corresponding tensile properties are reported in Table 2 [tensile modulus E_t , yield stress σ_y and tensile elongation at break ϵ_b (ultimate strain)]. Neat PLA exhibits a purely brittle tensile failure and behavior characterized by a high tensile modulus (1860 MPa), a high yield point (63 MPa) and a very low elastic axial deformation <6%. Indeed, neat PLA reveal crazes, whose propagation and coalescence can lead to the specimen fracture. It is well established that the macroscopic stresses that are dissipated locally may be due to a competition between damage mechanisms by crazing and chain orientation mechanisms. For neat PLA, the chain motion is definitely not high enough to initiate stress dissipation by chain orientation [26, 27]. Damage mechanisms are thus favored. Damage mechanisms are generally observed in brittle polymer below its brittle-to-ductile transition temperature [43].

All plasticized PLA specimens exhibit lower tensile modulus, lower yield stress, and higher strain at break as compared to neat PLA. Furthermore, all plasticized PLA specimens yielded stable necking, showing cold-drawing behavior. They were subjected to tensile deformation accompanied by whitening of the specimen due to the development of crazes in the amorphous phase, highlighting the plasticizing efficiency of ECard. Nevertheless, the plasticizing effect is very much dependent on the presence and the amount of the catalyst (reactivity of the materials). In fact, the reactive blend containing the lowest amount of catalyst, *i.e.*, 0.02 phr, exhibited the highest ductility behavior characterized with lower tensile modulus and higher strain at break. Indeed, the tensile modulus and the strain at break measured for PLA/ECard/ETPB-0.02 phr are 1110 MPa and 49%, while those displayed for the physical blend PLA/ECard and for the most reactive blend PLA/ECard/ETPB-0.06 phr are 1361 MPa and 32%, and 1425 MPa and 11%, respectively. Further increase of the amount of the catalyst has tendency to deteriorate the overall mechanical properties of the material. The same trend was observed by DMA. As mentioned above, ECard, being a difunctional glycidyl ether epoxy cardanol, crosslinking/branching reactions should take place simultaneously between the epoxy groups of the plasticizer and the carboxyl and hydroxyl end groups of PLA chains during reactive extrusion. As a consequence, the tensile/elastic modulus in the reactive blend PLA/ECard/ETPB-0.06 phr increases (Scheme 1).

Unlike neat PLA, in all plasticized PLA specimens molecular relaxation is enhanced and the stresses are dissipated by conformational changes of glassy amorphous PLA chains, leading to segmental orientation and disentanglement [26, 27]. These phenomena are more prominent in the reactive blend containing the lowest content of catalyst, that is, PLA/ECard/ETPB-0.02 phr blend.

CONCLUSIONS

In this study, plasticization of PLA with a new biobased plasticizer, di-functional glycidyl ether epoxy cardanol, is described. *In situ* reactive grafting strategy has been employed to improve the compatibility between PLA and ECard in presence of ETPB as a catalyst using twin-screw extruder. In absence of catalyst, ECard forms micron-sized domain dispersed in the PLA matrix. The weakness of the interface between PLA and ECard highlights a high incompatibility between both phases. Domain size distribution of the plasticizer decreases in presence of ETPB. This decrease is accentuated with the increase of the catalyst amount. This morphological trend can be explained by the fact that the reactive grafting of a fraction of ECard plasticizer onto PLA backbone leads to the creation of more interactions between the so-functionalized polyester matrix and the remaining fraction of non-grafted plasticizer. Although all plasticized PLA specimens exhibit lower glass transition temperature, lower elastic/tensile modulus, lower yield stress, and higher strain at break, the reactive blend containing the lowest amount of catalyst, that is, 0.02 phr, exhibited the highest ductility behavior. Indeed, it is clearly demonstrated in this study that at higher catalyst content (>0.02 phr), PLA chain scission and crosslinking/branching reactions occur, therefore deteriorating the overall properties of PLA based materials.

REFERENCES

1. D. Garlotta, *J. Polym. Environ.*, **9**, 63 (2001).
2. L.T. Lim, R. Auras, and M. Rubino, *Prog. Polym. Sci.*, **33**, 820 (2008).
3. I. Vroman, and L. Tighzert, *Materials*, **2**, 307 (2009).
4. R. Auras, B. Harte, and S. Selke, *Macromol. Biosci.*, **4**, 835 (2004).
5. H.N. Rabetafika, M. Paquot, and P. Dubois, *Biotechnol. Agronomie Soc. Environ.*, (2006).
6. C.J. Weber, V. Haugaard, R. Festersen, and G. Bertelsen, *Food Addit. Contam.*, **19**, 172 (2002).
7. K. Anderson, K. Schreck, and M. Hillmyer, *Polym. Rev.*, **48**, 85 (2008).
8. G. Kfoury, J.-M. Raquez, F. Hassouna, P. Leclère, V. Toniazzo, D. Ruch, and P. Dubois, *Polym. Eng. Sci.*, **55**, 1408 (2015).
9. H. Liu, and J. Zhang, *J. Polym. Sci. Part B: Polym. Phys.*, **49**, 1051 (2011).
10. G. Kfoury, J.M. Raquez, F. Hassouna, J. Odent, V. Toniazzo, D. Ruch, and P. Dubois, *Front. Chem.*, **1**, 32 (2013).
11. L. Mascia, and M. Xanthos, *Adv. Polym. Technol.*, **11**, 237 (1992).
12. P.R. Gruber, J.J. Kolstad, C.M. Ryan, R.S.E. Conn, and E.S. Hall, U.S. Patent 6,355,772 (2002).
13. R.G. Sinclair, U.S. Patent 5,180,765 (1993).
14. S. Jacobsen, and H.G. Fritz, *Polym. Eng. Sci.*, **39**, 1303 (1999).
15. N. Ljungberg, and B. Wesslén, *Biomacromolecules*, **6**, 1789 (2005).
16. W.M. Gramlich, M.L. Robertson, and M.A. Hillmyer, *Macromolecules*, **43**, 2313 (2010).
17. S. Vijayarajan, S.E.M. Selke, and L.M. Matuana, *Macromol. Mater. Eng.*, **299**, 622 (2014).
18. E. Azwar, B. Yin, and M. Hakkarainen, *J. Chem. Technol. Biotechnol.*, **88**, 897 (2013).

19. C.M. Buchanan, N.L. Buchanan, K.J. Edgar, and J.L. Lambert, U.S. Patent 2003171458 A1, (2003).
20. L. Dobircou, N. Delpouve, R. Herbinet, S. Domenek, L. Le Pluart, L. Delbreilh, V. Ducruet, and E. Dargent, *Polym. Eng. Sci.*, **55**, 858 (2015).
21. Z. Kulinski, E. Piorowska, K. Gadzinowska, and M. Stasiak, *Biomacromolecules*, **7**, 2128 (2006).
22. H. Zhang, J. Fang, H. Ge, L. Han, X. Wang, Y. Hao, C. Han, and L. Dong, *Polym. Eng. Sci.*, **53**, 112 (2013).
23. K. Okamoto, T. Ichikawa, T. Yokohara, and M. Yamaguchi, *Eur. Polym. J.*, **45**, 2304 (2009).
24. N. Ljungberg, and B. Wesslén, *Polymer*, **44**, 7679 (2003).
25. N. Ljungberg, T. Andersson, and B. Wesslén, *J. Appl. Polym. Sci.*, **88**, 3239 (2003).
26. F. Hassouna, J.M. Raquez, F. Addiego, P. Dubois, V. Toniazio, and D. Ruch, *Eur. Polym. J.*, **47**, 2134 (2011).
27. F. Hassouna, J.M. Raquez, F. Addiego, V. Toniazio, P. Dubois, and D. Ruch, *Eur. Polym. J.*, **48**, 404 (2012).
28. G. Kfoury, F. Hassouna, J.-M. Raquez, V. Toniazio, D. Ruch, and P. Dubois, *Macromol. Mater. Eng.*, **299**, 583 (2014).
29. G. Vasapollo, G. Mele, and R. Del Sole, *Molecules*, **16**, 6871 (2011).
30. E. Bloise, L. Carbone, G. Colafemmina, L. D'Accolti, S.E. Mazzetto, G. Vasapollo, and G. Mele, *Molecules*, **17**, 12252 (2012).
31. F. Jaillet, E. Darroman, A. Ratsimihety, R. Auvergne, B. Boutevin, and S. Caillol, *Eur. J. Lipid Sci. Technol.*, **116**, 63 (2014).
32. J. Chen, Z. Liu, J. Jiang, X. Nie, Y. Zhou, and R.E. Murray, *RSC Adv.*, **5**, 56171 (2015).
33. M. Alexander, and E.T. Thachil, *J. Appl. Polym. Sci.*, **102**, 4835 (2006).
34. F. Hassouna, I. Mihai, L. Fetzer, T. Fouquet, J.-M. Raquez, A. Laachachi, H. Ibn Al Ahrach, and P. Dubois, *Macromol. Mater. Eng.*, **301**, 1267 (2016).
35. Y. Li, and H. Shimizu, *Eur. Polym. J.*, **45**, 738 (2009).
36. H.T. Oyama, T. Kitagawa, T. Ougizawa, T. Inoue, and M. Weber, *Polymer*, **45**, 1033 (2004).
37. T. Fouquet, L. Fetzer, G. Mertz, L. Puchot, and P. Verge, *RSC Adv.*, **5**, 54899 (2015).
38. P. Verge, T. Fouquet, C. Barrère, V. Toniazio, D. Ruch, and J.A.S. Bomfim, *Compos. Sci. Technol.*, **79**, 126 (2013).
39. R. Pantani, F. De Santis, A. Sorrentino, F. De Maio, and G. Titomanlio, *Polym. Degrad. Stab.*, **95**, 1148 (2010).
40. K.I. Ku Marsilla, and C.J.R. Verbeek, *Eur. Polym. J.*, **67**, 213 (2015).
41. J.L. Halary, F. Laupretre, and L. Monnerie, *Polymer Materials: Macroscopic Properties and Molecular Interpretations*, Wiley, Hoboken, NJ (2011).
42. E. Piorowska, Z. Kulinski, A. Galeski, and R. Masirek, *Polymer*, **47**, 7178 (2006).
43. W.G. Perkins, *Polym. Eng. Sci.*, **39**, 2445 (1999).